Bioinspired, Biomimetic and Nanobiomaterials
Volume 4 Issue BBN1
Bioinspired electrohydrodynamic ceramic patterning of curved metallic substrates
Nithyanandan *et al*.

ice | science

Pages 59–67 http://dx.doi.org/10.1680/bbn.14.00020
Memorial Issue Research Paper
Received 02/05/2014 Accepted 04/07/2014
Published online 11/07/2014
Keywords: bioinspired\ceramic\electrohydrodynamic\metallic\substrate

ice Institution of Civil Engineers publishing

Bioinspired electrohydrodynamic ceramic patterning of curved metallic substrates

1 **Anouska Nithyanandan** MEng
PhD Researcher, Department of Mechanical Engineering, University College London, London, UK

2 **Suntharavathanan Mahalingam** PhD
Research Associate, Department of Mechanical Engineering, University College London, London, UK

3 **Jie Huang** PhD
Lecturer of Biomaterials, Doctor, Department of Mechanical Engineering, University College London, London, UK

4 **Sarrawat Rehman** PhD
Principal Bioengineer, JRI Orthopaedics Ltd, Chapeltown, Sheffield, UK

5 **Edward Draper** PhD
Innovation Manager, JRI Orthopaedics Ltd, Chapeltown, Sheffield, UK

6 **Mohan Edirisinghe** DSc*
Bonfield Chair of Biomaterials, Department of Mechanical Engineering, University College London, London, UK

Template-assisted electrohydrodynamic atomisation (TAEA) has been used for the first time to pattern curved metallic surfaces. Parallel lines of ceramic titania (TiO_2) were produced on titanium substrates, convex and concave with diameters of ~25 mm, at the ambient temperature. Optimal results were obtained with 4 wt% TiO_2 in ethanol suspension deposited over 300 s during stable cone-jetting at 20 µl/min, 10kV and collection distance 80 mm. A high degree of control over pattern line width, interline spacing and thickness were achieved. Nanoindentation load-displacement curves were continuous for the full loading and unloading cycle, indicating good adhesion between pattern and substrate. At a loading rate of 1 µN/s and a hold time of 1 s, pattern hardness decreased as load increased up to 7 µN and remained at 0·1 GPa up to higher loads. Elastic modulus behaved similarly, and both were not sensitive to loading rate. The effect of heat treatment to further consolidate the patterned deposits was also investigated. Hardness of the patterns was not markedly affected by heating. This work shows that TAEA is highly controllable and compatible on a range of substrate geometries. Extending TAEA capabilities from flat to curved surfaces, enabling the bioactive patterning of different surface geometries, takes this technology closer to orthopaedic engineering applications.

1. Introduction

Modifying the surface of load-bearing biomedical implants and inserts with patterned deposits of bioactive materials can support cell proliferation and orientation, improving direct biological fixation.[1,2] Practically this results in increased functional service life of implants, and fewer revision surgeries for patients. Our patented template-assisted electrohydrodynamic atomisation (TAEA) spraying is a novel ambient temperature process that can be exploited to apply non-continuous deposits in a wide range of materials[3,4] and potentially incorporate biological agents and drugs during manufacture. In TAEA patterning, topography can be controlled by way of template choice. The biological benefit of such patterns, in particular preferential cellular response, over continuous coatings has also been established.[4] The development of TAEA for application on curved substrates is a natural progression of research, which has been exclusively on flat surfaces to date since its invention,[5,6] and is a key milestone towards commercial viability. This work aims to further develop TAEA for the application of bioceramic patterns onto curved titanium (Ti) substrates for the first time.

TAEA processing uses ground electrode configurations and templates with electrohydrodynamic atomisation spraying[7] to deposit well-defined patterns onto a substrate surface (see Figure 1). The process consists of a nozzle (needle) that is connected to a high-voltage power supply and a ground electrode. A suspension

***Corresponding author e-mail address:** m.edirisinghe@ucl.ac.uk

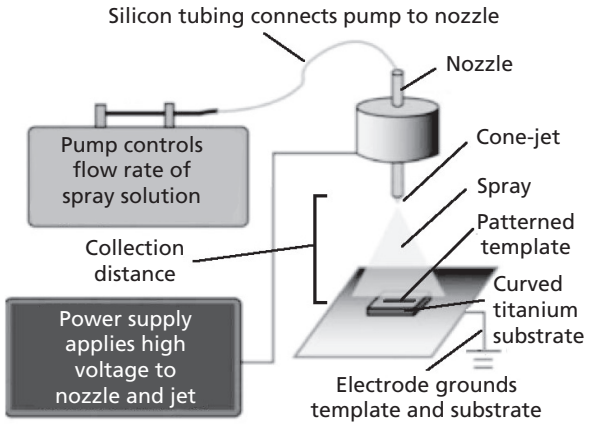

Figure 1. Schematic diagram of the TAEA process

or solution containing the desired coating material is fed through the nozzle (an electrode) at a controlled flow rate through a syringe pump. A copper template with the desired pattern is placed over the grounded substrate, which acts as one of the electrodes. The electric field created between the nozzle and the substrate forms a liquid jet at the nozzle exit. The jet eventually breaks up into fine and uniform droplets in the nano- or micrometre scale.[8] The droplets (spray) collect on the grounded substrate and template to produce a fine coating, the characteristics of which (e.g. droplet relic size) can be controlled by varying process parameters such as flow rate and applied voltage. After coating, the solvent evaporates and the template can be removed, leaving the inverted template pattern on the substrate.

There are not only similarities but also characteristic differences between flat and curved surface TAEA. The substrate, whether curved or flat, remains grounded; however, the collection distance between the needle and the top surface of a curved substrate varies with the curvature. This affects the electric polarisation stress parallel to the needle acting on the liquid meniscus on application of the electric potential. The relationship between collection distance and the dimensions of the liquid droplets is well documented in the literature.[8–10] As the collection distance increases, liquid droplet size decreases as the solvent carrier evaporates in transit, resulting in smoother coatings. As the collection distance decreases, liquid droplet size increases as less solvent carrier evaporates in transit, resulting in rougher coatings. This greatly affects the integrity and uniformity of resultant coatings. Therefore, increased collection (working) distances are preferable so that the difference in height across the substrate is less significant compared to the average collection distance.

The bioceramic hydroxyapatite (HA) is typically used when coating metal prostheses for controlled implant or tissue interfacial response. The mechanical behaviour of HA is acceptable when under low-load conditions and it exhibits excellent biocompatibility, although it degrades slowly in vivo.[11] However, applying a patterned layer of titania (TiO_2) before applying HA significantly improves interfacial adhesion, therefore the TAEA application of both TiO_2 and HA on curved Ti substrate warrants investigation.[12,13] In addition, TiO_2 coatings have been found to improve the corrosion resistance of titanium substrates[14] and thus their functionality in load-bearing orthopaedic applications.[15] The outer HA layer enhances the bioactivity and osteoconductivity initially, and the inner TiO_2 layer prevents the titanium substrate from corroding, even after the HA layer has completely resorbed into the body.[16] The TiO_2 pattern interlocks with the HA coating on the Ti substrate, in an enhanced manner in TAEA, and improves mechanical strength and chemical bonding, thus clinical functionality.[5]

In this work, we further develop and exploit TAEA for the application of predetermined TiO_2 patterns on curved Ti substrates for the first time. We show that this is indeed possible, with results comparable to that of existing research on exclusively flat substrates. However, further work is needed to scale-up the process to larger curved surfaces and substrates, and ongoing and future work will address this. The results obtained are verified by way of analysis of the pattern morphology, and mechanical testing by nanoindentation. A systematic study on the relationship between heating the patterns and their resultant mechanical properties was also carried out.

2. Experimental details

2.1 Materials

Titanium (IV) isopropoxide ($Ti(OCH(CH_3)_2)_4$) was purchased from Sigma-Aldrich (Poole, UK) and pure ethanol (99·7 wt%) from BDH laboratory Supplies (Poole, UK). The Ti substrate used for deposition was Grade 1 (ASTM F67) commercially pure Ti tubing (Advent Research Materials, Oxford, UK) of 0·5 mm thickness, which was cut lengthways to produce small curved plates that could have both the inner and outer surfaces prepared for coating. Convex (outer) diameter was 25·4 mm and concave (inner) diameter was 23·6 mm. Flat Ti plates for heated samples were obtained from Advent Research Materials. Copper templates (100 mesh copper, 3·05 mm) were purchased from Agar Scientific (Stansted, UK). Silicon carbide grinding paper No. 800, No. 1200, No. 2400 and No. 4000 were used to polish the substrate surface. All reagents were of analytical grade and were used as received.

2.2 Suspension preparation

Appropriate quantities of TiO_2 were mixed in ethanol. The weight ratios of TiO_2 to ethanol were as follows: (TiO_2: ethanol) 2:98, 4:96, 6:94, that is, 2, 4 and 6 wt% TiO_2 in ethanol, respectively. The suspensions were stirred mechanically (magnetic stirrer) for 60 min at the ambient temperature (20°C) to ensure the ceramic was homogeneously dispersed in the ethanol.

2.3 Suspension characterisation

All the equipments used to characterise the suspensions were calibrated using ethanol as a reference data at the ambient temperature

of 20°C. The density, viscosity, surface tension and electrical conductivity of the suspensions were measured. The density was measured using a standard 25 ml density bottle (VWR International, UK) using a high-precision scale (six decimal places). The surface tension was measured using a Kruss Tensiometer (A. Krüss Optronic GmbH, Hamburg, Germany) (Standard Wilhelmy's plate method). The viscosity of the TiO_2 suspensions was determined using a U-tube viscometer. The electrical conductivity was estimated using a HI-8733 Hanna Instruments probe (Hanna Instruments, Woonsocket, RI).

2.4 Patterning

The Ti plates were polished using silicon carbide grinding paper (up to No. 4000) for uniform surface roughness, and thoroughly cleaned with ethanol to remove contaminants. Copper templates with parallel-patterned mesh size with a strut width (width of template lines) of 50 µm and spacing (distance between edge of template lines/struts) of 100µm were used in all experiments. The template determined the architecture of the deposited pattern, and was placed on the Ti substrate. The needle and silicone tubing (Figure 1) were flushed with ethanol immediately prior to patterning to minimise contamination. For each experiment, the suspension was drawn into a 10-ml Becton-D plastic syringe (BD, Franklin Lakes, NJ) and secured in a high-precision Harvard syringe pump (Harvard Apparatus, Holliston, MA) that controls the infusion flow rate. The needle was made from stainless steel with an inner diameter of approximately 300 µm and was coupled to a high-voltage power supply (Glassman Europe Ltd., Tadley, UK). The substrate platform was grounded. The needle was subjected to controlled electric fields by increasing the applied voltage from 0 to 15 kV. Plastic shielding was used to guard the spray area from external electric fields and the atmosphere.

The suspensions were fed through the needle at controlled flow rates (5, 10, 15, 20 and 25 µl/min) from directly above the substrate platform. A camera was used to observe and characterise the jet and the jet break-up process. When a stable cone-jet spray had been achieved, the template was placed on the highest point of the convex substrate, or lowest point of the concave substrate, and the two were placed on top of the platform for coating. The distance between the tip of the needle and the template area on the substrate (collection distance) was maintained at 80 mm throughout the experiments to allow some of the solvent to evaporate before collecting on the substrate. This created a finer spray and more even pattern than at smaller collection distances. The time the substrate was coated (collection time) was also varied. All experiments were carried out at ambient temperature (~20°C).

2.5 Characterisation of patterns

The morphology and structure of the coatings were determined using optical microscopy (Zeiss Axiotech (Carl Zeiss AG, Oberkochen, Germany) fitted with a Nikon (Tokyo, Japan) Eclipse ME 600 camera OM) and scanning electron microscopy (JEOL (Tokyo, Japan) JSM-6301F field emission, SEM). Samples analysed using SEM were sputter-coated with gold for 120 s prior to examination, and analysis was conducted in the voltage range of 5–10 kV.

The width of the generated parallel line deposits (line width) was measured using standard OM and SEM images coupled to an imaging tool program, which allowed the mean measurements of geometric features to be calculated by way of direct link-up analysis of imaging and magnification. The dimension of the patterns in terms of width and gap was measured using image analysis where the number of measurements (n) = 50.

In order to compare the uniformity of the TAEA spraying across the curved substrate, mean line widths were measured at different points across the curve. These positions are shown in Figure 2. The Ti substrate was in the same position for all three experimental set-ups; it was only the template position that was varied. Comparing the mean width for each position will give an indication on how uniform the coating is across the curve. A mean closest to 100 µm (template width) indicates the most accurate templating, as the pattern exactly resembles the negative of the template. A mean that varies more greatly from the original template width indicates less accurate templating and more particle spread. In this way, the effect of template position on resultant microstructure can be assessed. This investigation is relevant because, for TAEA to be translated to curved surfaces, the resultant patterns need to be as homogenous as on flat surfaces.

2.6 Nanoindentation

Hardness and elastic modulus of the patterns were evaluated using nanoindentation techniques adopted in previous studies.[3] The nanoindentation tests were carried out in a Bruker–3100 AFM (Billerica, MA). A three-sided pyramidal Berkovich diamond indenter with a nominal tip radius of 10 nm was used throughout the experiments. The fused silica glass was used to calibrate the instrument before the measurements were recorded. The indentation load and the displacement were continuously recorded during one complete cycle of loading and unloading. The thermal drift of the transducer was corrected during each measurement. By invoking the Oliver–Pharr method, the hardness and the effective elastic modulus

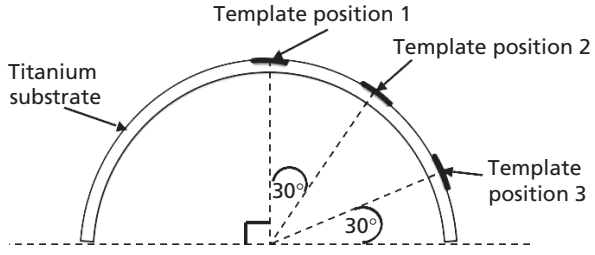

Figure 2. Schematic illustration of the three template positions for probing curved surface TAEA

Suspension	Density: kg/m³	Viscosity: mPa s	Surface tension: mN/m	Electrical conductivity: S/m
Ethanol	790	1·3	23	$0{\cdot}1 \times 10^{-4}$
1 wt% TiO_2 in ethanol	790	1·3	24	$0{\cdot}5 \times 10^{-4}$
2 wt% TiO_2 in ethanol	791	1·5	26	$0{\cdot}6 \times 10^{-4}$
4 wt% TiO_2 in ethanol	794	1·7	29	$0{\cdot}6 \times 10^{-4}$
6 wt% TiO_2 in ethanol	799	1·8	32	$0{\cdot}7 \times 10^{-4}$
8 wt% TiO_2 in ethanol	802	1·9	34	$0{\cdot}7 \times 10^{-4}$
10 wt% TiO_2 in ethanol	808	2·1	35	$0{\cdot}8 \times 10^{-4}$

Table 1. Suspension properties

were calculated from the unloading curve of the nanoindentation tests.[17] The effect of load, loading rate and the holding time on the mechanical properties of the TiO_2 patterns were studied.

One of the key benefits of TAEA over more common, high-temperature (15,000°C) industrial deposition techniques such as vacuum plasma spraying is that it can be carried out at ambient temperature. Therefore, the effect of heating the titanium dioxide deposits was investigated to ascertain whether further consolidation of the 'green' unsintered samples had an effect on hardness and elastic modulus of the patterns. Separate sets of TiO_2 TAEA-patterned flat Ti substrate samples (three used for each temperature) were heated to 100°C, 200°C, 300°C, 400°C, 500°C, 600°C, 700°C and 800°C, from ambient temperature at a ramp rate of 1°C/min, and cooled slowly back to ambient temperature by way of annealing. They were then analysed by way of nanoindentation in the same way as the initial, unheated patterns, and the hardness and elastic modulus were recorded.

3. Results and discussion

3.1 Suspension properties

The TAEA process of producing the patterns is electric-field assisted; therefore it is controlled by both the processing parameters of the technique (such as flow rate and applied voltage) as well as the physical properties of the suspensions (such as density, viscosity, surface tension and electrical conductivity). A combination of processing parameters and physical properties determines the different jetting modes of the various suspensions.[8,18] Table 1 shows how the measured physical properties of the suspension vary with respect to concentration, from 100 wt% ethanol to 10 wt% TiO_2 in ethanol. Results for ethanol were verified with the literature.[19]

The electrical conductivities of the suspensions were in the range $0{\cdot}1–0{\cdot}8 \times 10^{-4}$S/m. TiO_2 addition caused the density to increase by 2%. However, viscosity and surface tension increased by 62% and 52%, respectively, with the addition of 10 wt% TiO_2. This affects the ability and readiness of the suspension material to achieve stable jetting under the influence of an electric field. Therefore, it

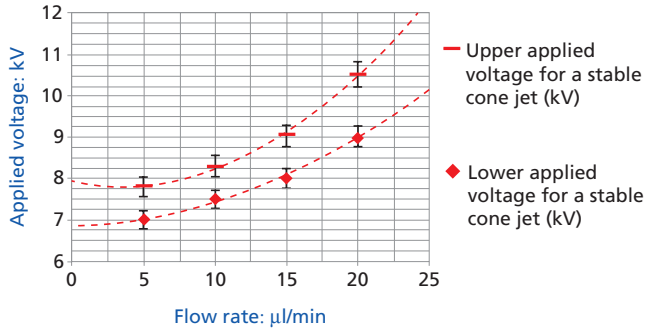

Figure 3. Applied voltage variation with flow rate for 4 wt% TiO_2 for stable-cone-jet mode electrohydrodynamic atomisation jetting with collection distance of droplets maintained at 80 mm

was found that 2–4 wt% TiO_2 was ideal for coating in the stable-cone jet mode (not too viscous but electrically conductive enough), which is necessary to generate homogeneous droplets.

The voltage–flow rate map for 4 wt% TiO_2 (Figure 3) was also plotted as a reference for obtaining a stable-cone jet under different conditions. It was found that at a flow rate increased from 5 to 20 µl/min, the applied voltage window for stable-cone jetting increased from 0·75 to 1·5 kV, that is, it doubled in range. This made stable-cone jetting easier to achieve at a 20 µl/min flow rate.

3.2 Pattern geometry

During stable jetting, the spray coats the template and the substrate as they are both grounded. This is essential in creating uniform coatings across the substrate so that after spraying, the template can be removed to leave an even pattern. Figure 4 shows the development of the coatings, from the parallel copper template, the coated template and resultant coating observed by way of OM and SEM. The resultant patterns show that the template dimensions influence the geometry of the coatings, so they can be chosen to meet the specific clinical needs of the coating. A clear correlation between the template shape and size and the achieved pattern was established. It was observed that the coating adhered well to

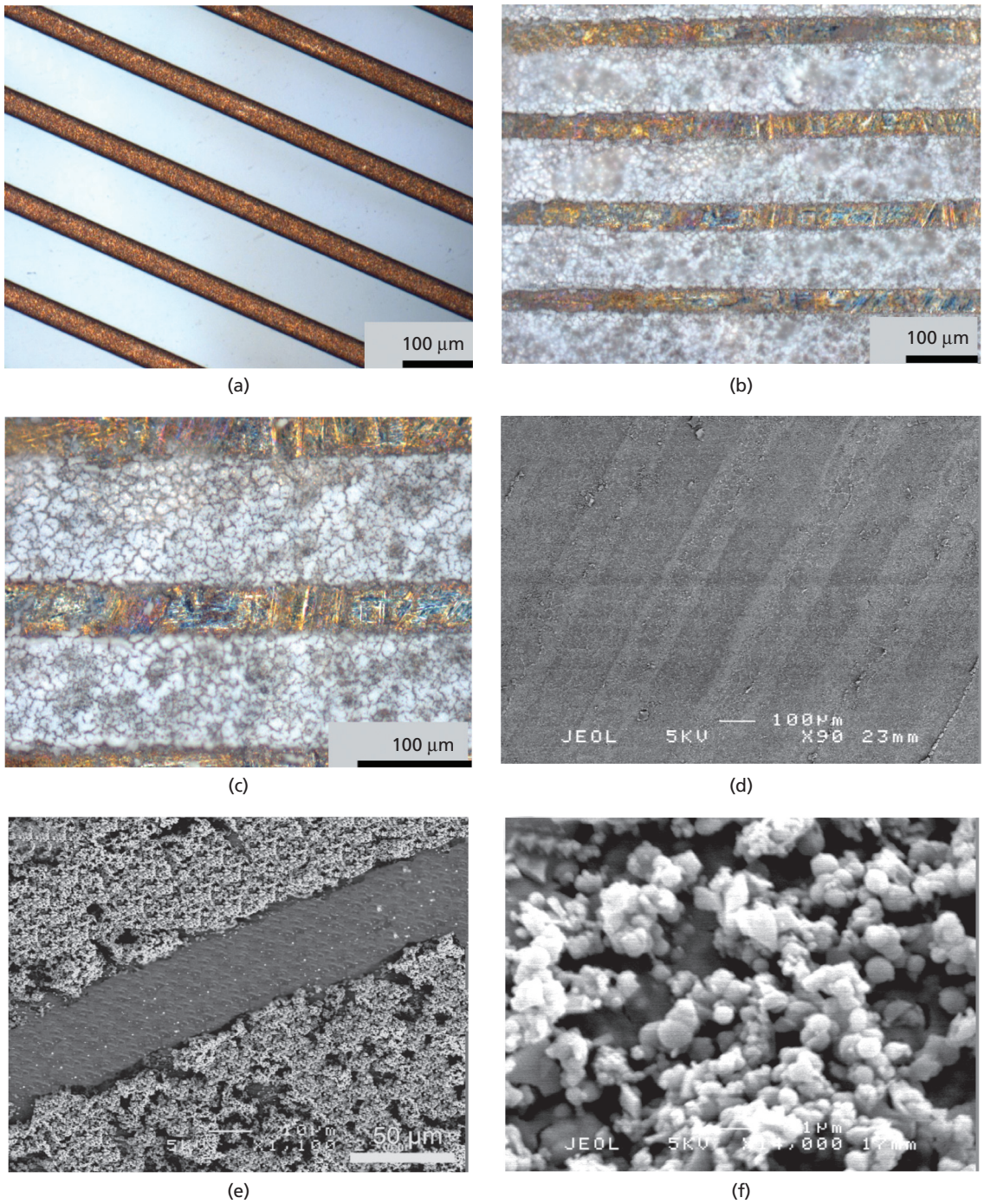

Figure 4. Optical micrographs of: (a) parallel copper template with strut width of 50 µm and inter-strut spacing of 100 µm. (b) TiO_2 pattern on curved Ti substrate. (c) pattern at greater magnification. (d)–(f) show scanning electron micrographs of TiO_2 pattern. All images depict spraying of suspension 4 wt% TiO_2 with flow rate, applied voltage and collection time 20 µl/min, 10 kV and 300 s, respectively, and convex substrate is Ti of diameter 25·4 mm.

the metal substrate because, on template removal, the boundary between coated and uncoated substrate was well defined (see Figure 4(e) and discussion under nanoindentation results). Varying the spraying time can control the height of the patterns, but this is a trade-off with the narrowness of the patterned lines. Figure 4 also shows that TiO_2 patterns have been sprayed onto curved Ti substrates with uniform and ordered topography. Results for the parallel template (with strut width of 50 µm, spacing of 100 µm)

show that the mean distance between patterned lines (interline spacing) is 54 µm and the mean line width is 97 µm (standard deviation 6 µm and 12 µm, respectively). This was achieved when 4 wt% TiO_2 was applied by way of TAEA at a flow rate of 20 µl/min, applied voltage of 10 kV, collection distance 80 mm and collection time of 300 s.

The same template shape was used for all experiments so the shape and size of patterns across the entire coating were kept constant. Since the collection time was controlled at 300 s during the process, the height of the patterns (normal to the substrate surface) was kept approximately constant (42 ± 5 µm measured by way of SEM image analysis). Figure 4(f) shows that the coatings exhibit a microporous surface, with pore less than 1 µm in diameter. This is beneficial for cell attachment and enhances bioactivity.[20]

3.3 Effect of substrate curvature on patterning

In order to compare the uniformity of the TAEA spraying across the curved substrate, mean line widths were measured at different points across the curve (see Figure 2). Figure 5 shows how optimal results were obtained at Position 1, as the mean deposit width was measured as 98 µm, closest to the actual template size (100 µm). Figure 5 also shows that Position 1 yielded minimum spread as the standard deviations of both measures were lowest here. Position 1 was at the top of the curved substrate, thus the pattern surface was most parallel to the grounded platform compared with Positions 2 and 3, and means that results were most comparable to TAEA of flat substrates.

As the template position increased from 1 to 3, the angle at which the patterning area lays also increased. Results showed that as this angle increased, mean deposit width decreased to 96 µm (by 2%) and mean spacing width increased from 53 to 55 µm (by 4%). Spread (standard deviation) increased for both parameters. This indicates that curvature does affect the uniformity of TAEA patterning, but at these diameters, not greatly. Further work will investigate how this phenomenon varies as curved surface diameter also varies from convex diameter 25·4 mm and concave diameter 23·6 mm.

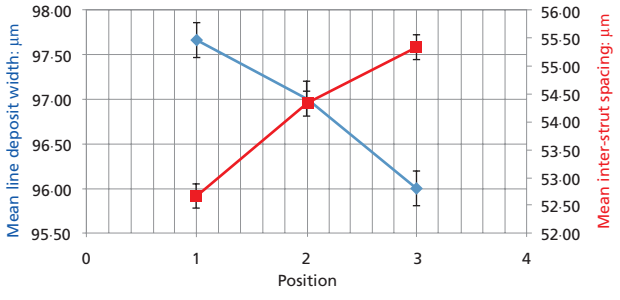

Figure 5. Mean deposit width and spacing variation with position on substrate curve. Error bars depict standard deviation.

3.4 Pattern adhesion and properties

A typical load–displacement curve obtained during the nanoindentation on bioceramic TiO_2 pattern is shown in Figure 6(a). The continuous curve for the complete cycle of loading and unloading indicates good adhesion of the patterns to the substrate.[17] This also suggests no cracking or delamination of the TiO_2 pattern on the substrate. The hardness of the ceramic patterns was calculated from the maximum load (P_{max}) and the contact area of the indentation (A).[21]

$$1. \qquad H = \frac{P_{max}}{A}$$

A was calculated using the following equation[22]:

$$2. \qquad A = 24 \cdot 5h_c^2$$

where h_c represents the contact depth as measured at the maximum load.

The effective elastic modulus was derived from the initial slope of the unloading cycle (S, stiffness) and the contact area of the indentation (A).[23]

$$3. \qquad E_r = \frac{\sqrt{\pi}}{2}\frac{S}{A}$$

Figure 6(b) shows the effect of load on the TiO_2 patterns at a loading rate of 1 µN/s and a hold time of 1 s. Hardness decreases as load increases up to 7 µN, and then remains at that value (0·1 GPa) up to higher loads. Elastic modulus also decreases up to ~10 µN, and then remains at that value (0·3 GPa) up to higher loads. This decrease in hardness and effective elastic modulus can be attributed to the microporosity observed in the TiO_2 deposits, as higher loads are able to penetrate more easily into microporous structures. This supports the results of[24] other coatings. Although adhesion as a function of time (storage) has not been considered in this work, there is no reason to believe that adhesion will deteriorate with time. Experimental verification of this fact is important in future exploitation of this process.

The hardness and effective elastic modulus of TiO_2 patterns with regard to loading rate were analysed and shown in Figure 6(c). The hardness was 7·5 GPa at a loading rate of 0·1 µN/s, and reduced to 7·3 GPa when the loading rate was increased to 1 µN/s. This is only a 2% decrease, so it can be concluded that hardness is not significantly affected by loading rate within these testing limits. This means that the TiO_2 exhibits brittle properties (as expected for ceramic materials), which is why the hardness value did not change. With respect to effective elastic modulus, this was found to be 7·5 GPa at a loading rate of 0·1 µN/s, and reduced to 7·3 GPa when the loading rate was increased to 1 µN/s. This again is a 2% decrease, so it can be concluded that elastic modulus is also

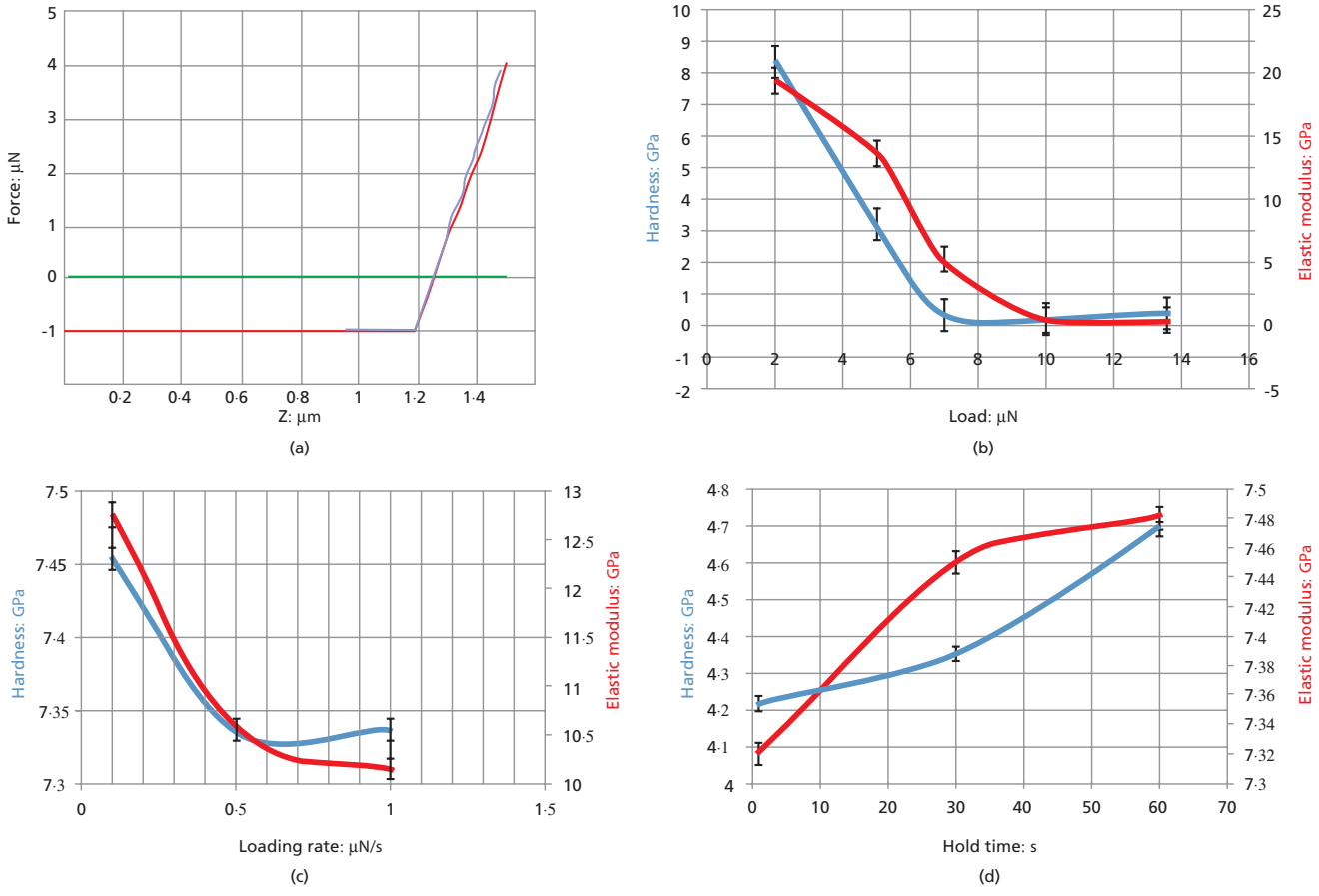

Figure 6. (a) A typical load–displacement curve obtained from the nanoindentation tests on TAEA TiO_2 pattern with a loading rate of 1 µN/s. Variation of hardness and effective elastic modulus with (b) load, (c) loading rate and (d) hold time.

not significantly affected by loading rate within these parameters. This shows that both hardness and effective elastic modulus are not sensitive to loading rate.

The variation of hardness and the effective elastic modulus with hold time is shown in Figure 6(d). Both parameters increased as hold time increased from 1 to 60 s by 12% and 24%, respectively. This indicates that longer hold times allowed for more energy to be dissipated across the specimen sample as high values were found for both parameters.

3.5 Heat-treated TAEA deposits

Figure 7 shows that hardness is not significantly affected by post-pattern heating to consolidate the TiO_2 on the metallic substrate, as this increases by only 5·2% from 100°C to 800°C. In fact, the elastic modulus reduces by 2·8% on heating to ~500°C and then remains comparatively unaffected. Future work will investigate the co-feeding of other bioactive species during TAEA as this is easily accommodated if co-axial nozzles are used (Figure 1). However, if

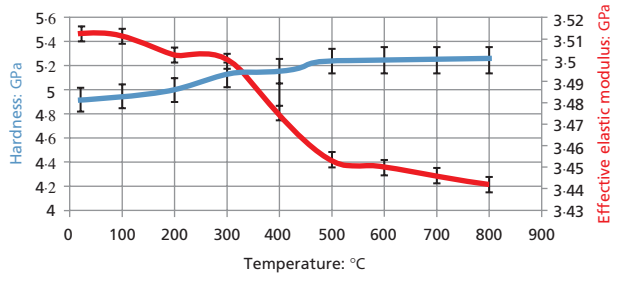

Figure 7. Variation of hardness and effective elastic modulus with heat treatment temperature from 20°C (ambient temperature, i.e. no heat treatment) to 800°C. Load is 5 µN, loading rate is 1 µN/s. Values are means of three separate samples.

other organic bioactive species are included in the TAEA process at ambient temperature, post-deposition heating is to be avoided as it can lead to the degradation of these species. Therefore it is encouraging that the results in Figure 7 do not show marked mechanical property

enhancement by post-deposition heat treatment, although this aspect will be further investigated in ongoing work.

4. Conclusions

A method of producing TiO_2 patterns on curved Ti substrates by way of the TAEA process has been developed with a high degree of control over the pattern geometry (by way of template choice) and thickness (by way of collection time). TiO_2 patterns with parallel lines have been successfully produced on both convex and concave Ti substrate diameters of ~25 mm. Optimal results were obtained with 4 wt% TiO_2 in ethanol suspension sprayed within the stable-cone-jet mode window at a flow rate of 20 µl/min for 300 s at 10 kV with a collection distance of 80 mm.

A clear correlation between the template shape and size and the achieved pattern was established, therefore the template can be chosen to reflect the specific clinical needs of the coating. Results for the parallel template (with strut width of 50 µm, spacing of 100 µm) show that the mean interline spacing is 54 ± 6 µm and the mean line width is 97 ± 12 µm. Since the collection time was controlled at 300 s during the process, the height of the patterns (normal to the substrate surface) was kept approximately constant at 42 ± 5 µm.

For TiO_2 patterns at a loading rate of 1µN/s and a hold time of 1 s, hardness decreases as load increases up to 7 µN and remains at 0·1 GPa up to higher loads. Elastic modulus behaves in a similar way. This decrease can be attributed to the microporosity observed in the TiO_2 deposits as higher loads are able to penetrate more easily into microporous structures. Hardness is 7·5 GPa at a loading rate of 0·1 µN/s, and reduces to 7·3 GPa when the loading rate is increased to 1 µN/s. This is only a 2% decrease, thus the hardness is not significantly affected by the loading rate due to the brittle nature of the TiO_2 ceramic. With respect to effective elastic modulus, this is found to be 7·5 GPa at a loading rate of 0·1 µN/s, and reduces to 7·3 GPa when the loading rate is increased to 1 µN/s. This again is a 2% decrease, so we can conclude that elastic modulus is also not significantly affected by loading rate within these parameters. Post-patterning heat treatment does not show marked enhancement of deposit mechanical properties and, although this requires more intensive investigation on curved surface TAEA samples, is a positive finding in terms of incorporating other temperature-sensitive bioactive species by extending forming and stage to co-axial electrohydrodynamics.

Ongoing work is also focused on the production of interlocked HA–TiO_2 patterns on a variety of biomaterial surfaces, in order to bring his technology closer to orthopaedic and other biomedical applications.

This work shows that the TAEA process is highly controllable and compatible on a range of substrate geometries, including flat, concave and convex substrates. Due to the versatile nature of the process, TAEA could provide increased capabilities for the coating of biomedical implants.

Acknowledgements

The authors would like to thank University College London (UCL) and JRI Orthopaedics Ltd for supporting this work and the doctoral research work of Anouska Nithyanandan. A 2013 Royal Society Brian Mercer Feasibility Award and the funding from the Engineering and Physical Sciences Research Council of the United Kingdom (Grant EP/L 024225/1) are also gratefully acknowledged.

REFERENCES

1. Overgaard, S. Calcium phosphate coatings for fixation of bone implants: evaluated mechanically and histologically by stereological methods. *Acta Orthopaedica Scandinavica* **2000**, *71* (Supplementum 297), 1–74.
2. Wang, W.; Ouyang, Y. H.; Poh, C. K. Orthopaedic implant technology: biomaterials from past to future. *Annals Academy of Medicine Singapore* **2011**, *40* (5), 237–244.
3. Nithyanandan, A.; Mahalingam, S.; Huang, J., et al. Template-assisted electrohydrodynamic atomization of polycaprolactone for orthopedic patterning applications. *Materials Science and Engineering: C* **2013**, *33*, 4608–4615.
4. Munir, G.; Koller, G.; Di Silvio, L., et al. The pathway to intelligent implants: osteoblast response to nano silicon-doped hydroxyapatite patterning. *Journal of the Royal Society Interface* **2011**, *8* (58), 678–688.
5. Li, X.; Huang, J.; Ahmad, Z.; Edirisinghe, M. Electrohydrodynamic coating of metal with nano-sized hydroxyapatite. *Bio-Medical Materials and Engineering* **2007**, *17* (6), 335–346.
6. Li, X.; Koller, G.; Huang, J., et al. A novel jet-based nano-hydroxyapatite patterning technique for osteoblast guidance. *Journal of the Royal Society Interface* **2010**, *7* (42), 189–197.
7. Leeuwenburgh, S. C. G.; Heine, M. C.; Wolke, J. G. C., et al. Morphology of calcium phosphate coatings for biomedical applications deposited using Electrostatic Spray Deposition. *Thin Solid Films* **2006**, *503* (1–2), 69–78.
8. Jaworek, A.; Krupa, A. Classification of the modes of EHD spraying. *Journal of Aerosol Science* **1999**, *30* (7), 873–893.
9. Hartman, R. P. A.; Brunner, D. J.; Camelot, D. M. A.; Marijnissen, J. C. M.; Scarlett, B. Jet break-up in electrohydrodynamic atomization in the cone-jet mode. *Journal of Aerosol Science* **2000**, *31* (1), 65–95.
10. Enayati, M.; Ahmad, Z.; Stride, E.; Edirisinghe, M. Size mapping of electric field-assisted production of polycaprolactone particles. *Journal of the Royal Society Interface* **2010**, *7*, S393–S402.
11. Paital, S. R.; Dahotre, N. B. Calcium phosphate coatings for bio-implant applications: materials, performance factors, and methodologies. *Materials Science and Engineering R* **2009**, *66* (1–3), 1–70.

12. Kim, H. W.; Knowles, J. C.; Kim, H. E. Hydroxyapatite/poly(epsilon-caprolactone) composite coatings on hydroxyapatite porous bone scaffold for drug delivery. *Biomaterials* **2004**, *25* (7–8), 1279–1287.
13. Lin, C. M.; Yen, S. K. Characterization and bond strength of electrolytic HA/TiO_2 double layers for orthopaedic applications. *Journal of Materials Science: Materials in Medicine* **2005**, *16* (10), 889–897.
14. Cabrini, M.; Cigada, A.; Rondelli, G.; Vicentini, B. Effect of different surface finishing and of hydroxyapatite coatings on passive and corrosion current of Ti6Al4V alloy in simulated physiological solution. *Biomaterials* **1997**, *18* (11), 783–787.
15. Kurzweg, H.; Heimann, R. B.; Troczynski, T.; Wayman, M. L. Development of plasma-sprayed bioceramic coatings with bond coats based on titania and zirconia. *Biomaterials* **1998**, *19* (16), 1507–1511.
16. Munir, G.; Huang, J.; Edirisinghe, M.; Nangrejo, M. R.; Bonfield, W. Electrohydrodynamic processing of calcium phosphates: coating and patterning for medical implants. *Nano LIFE* **2012**, *2*, 1–17.
17. Bhushan, B.; Li, X. D. Nanomechanical characterisation of solid surfaces and thin films. *International Materials Reviews* **2003**, *48* (3), 125–164.
18. Sebbowa, T.; Edirisinghe, M.; Salih, V.; Huang, J. Effect of deposition parameters and post-deposition annealing on the morphology and cellular response of electrosprayed TiO_2 films. *Biofabrication* **2011**, *3* (4), 045001.
19. Grace, J. M.; Marijnissen, J. C. M. A review of liquid atomization by electrical means. *Journal of Aerosol Science* **1994**, *25* (6), 1005–1019.
20. Lewandrowski, K. U.; Bondre, S. P.; Wise, D. L.; Trantolo, D. J. Enhanced bioactivity of a poly(propylene fumarate) bone graft substitute by augmentation with nano-hydroxyapatite. *Bio-Medical Materials and Engineering* **2003**, *13* (2), 115–124.
21. Oliver, W. C.; Pharr, G. M. An improved technique for determining hardness and elastic-modulus using load and displacement sensing indentation experiments. *Journal of Materials Research* **1992**, *7* (6), 1564–1583.
22. Malzbender, J.; den Toonder, J. M. J.; Balkenende, A. R.; de With, G. Measuring mechanical properties of coatings: a methodology applied to nano-particle-filled sol-gel coatings on glass. *Materials Science and Engineering R* **2002**, *36* (2–3), 47–103.
23. Zhou, J.; Komvopoulos, K. Surface and interface viscoelastic behaviors of thin polymer films investigated by nanoindentation. *Journal of Applied Physics* **2006**, *100* (11), 114329-1–114329-8
24. Fang, T. H.; Chang, W. J. Nanoindentation characteristics on polycarbonate polymer film. *Microelectronics Journal* **2004**, *35* (7), 595–599.

WHAT DO YOU THINK?

To discuss this paper, please email up to 500 words to the managing editor at bbn@icepublishing.com

Your contribution will be forwarded to the author(s) for a reply and, if considered appropriate by the editor-in-chief, will be published as a discussion in a future issue of the journal.

ICE Science journals rely entirely on contributions sent in by professionals, academics and students coming from the field of materials science and engineering. Articles should be within 5000-7000 words long (short communications and opinion articles should be within 2000 words long), with adequate illustrations and references. To access our author guidelines and how to submit your paper, please refer to the journal website at www.icevirtuallibrary.com/bbn